P-620

May 4, 1979

Proposal to Measure the Magnetic Moments Of The Σ^+, Ξ^-, Σ^-, and Ω^- Hyperons Using The Fermilab Neutral Hyperon Beam

L. Pondrom,* R. Handler, R. March, and M. Sheaff
University of Wisconsin, Madison

T.J. Devlin, A. Beretvas, and R. Whitman
Rutgers, The State University of New Jersey

O.E. Overseth
University of Michigan

K. Heller
University of Minnesota

Summary

A high flux polarized charged hyperon beam can be built in the M-2 line of the Meson Laboratory by inserting a curved channel in the neutral hyperon sweeping magnet. The standard hyperon spectrometer and lead glass array, augmented by upstream drift chambers to detect the incident charged hyperon direction will be used to observe decays $\Sigma^+ \to p\pi^\circ$, $\Xi^- \to \Lambda\pi^-$, $\Sigma^- \to n\pi^-$, and $\Omega^- \to \Lambda K^-$. One hundred fifty hours of data in the positive beam and 150 hours in the negative beam will yield errors in the anomaly a = (g/2 - 1) of $\delta a\ (\Sigma^+) = \pm.013$, $\delta a\ (\Xi^-) = \pm.02$, $\delta a\ (\Sigma^-) = \pm.10$, and $\delta a\ (\Omega^-) = \pm.4$, assuming an average polarization $\langle P \rangle = .08$ for each hyperon.

* 608-262-2281

I. Polarization

The discovery of inclusive hyperon polarization in the reaction $p + Be \rightarrow \Lambda + X$ in the Fermilab neutral hyperon beam has made possible a precise measurement of the Λ magnetic moment.[1] The Λ polarization increases monotonically with increasing $p_\perp$ for $0 \leq p_\perp \leq 2$ GeV/c.[2] At constant $p_\perp$, the polarization increases slightly with increasing $x = p^*_{\parallel}/p^*_{\parallel max}$. P_Λ $(x, p_\perp)$ is slightly larger from hydrogen than from beryllium.[3] The kinematic behavior is consistent with a "leading particle" effect, where the incident proton becomes polarized via some exchange mechanism which changes it into a forward going Λ. Ξ° hyperons, while produced only about 1% as often as Λ's, are also polarized.[4] Preliminary results from E-495 show that the magnitude, sign, and kinematic dependence of P_{Ξ° are consistent with that of P_Λ.[5] The existence of a non-zero P_{Ξ° led naturally to a measurement of the hitherto unknown magnetic moment of the Ξ°.[4] This work is continuing, and μ_{Ξ° will be known to about 1% accuracy when the analysis of E-495 is completed.

While P_Λ and P_Ξ are non-zero, there is no evidence for a polarization of $\bar{\Lambda}$'s in the same kinematic region.[2] Since $\bar{\Lambda}$'s originate via baryon - anti-baryon pair production, a process quite different from a leading particle exchange effect, it is perhaps not surprising that they are not polarized. There is no evidence that inclusively produced protons are polarized,[6] but the incident proton does not have to change any quantum numbers to become an out going proton, and the diffractive contribution dilutes the polarization that may arise from other channels.

Although there is no experimental evidence that charged hyperons are polarized, it seems highly likely that they are. Certainly the polarization of Ξ^- is strongly implied by that of the Ξ°, and the $\Sigma^\pm$ are probably polarized in a manner similar to the Λ. The Ω^-, produced at the target at the level of about 1% of the Ξ^-,[7] are quite rare, and are less certain to be polarized, (spin 3/2 is one complication) but come along "for free" in the Ξ^- sample, and hence will be analyzed just in case.

II. Magnetic Moments

Table I shows the current experimental status of the baryon magnetic moments, together with the predictions based on the simple broken SU_6 quark model. In the calculations it was assumed that $\mu_u/\mu_d = -2$, the same as the charge ratio, and that $\mu_s = \mu_\Lambda$. The moments of the quarks were calculated from the proton and Λ magnetic moments, and these quark moments were then used to predict the magnetic moments of the other baryons. The quark mass ratio m_s/m_u calculated from the equation $m_s/m_u = -1/2\ \mu_u/\mu_s$

agrees very well with the result obtained by DeRujula, et al.[8] who computed the same ratio from experimental mass difference ratios between different mesons and baryons. The quark masses themselves can be calculated from the magnetic moments μ_u and μ_s by assuming g = 2. The results are $m_u = m_d = 336$ MeV/c^2, and $m_s = 513$ MeV/c^2. In the language of the quark model these are "constituent" quark masses, as opposed to the appropriate masses for "free" quarks or "current" quarks.

The significance of the close agreement between constituent quark masses calculated from mass splittings of the particles and those calculated from magnetic moments has been discussed by Lipkin.[9] The problem of quark mass, namely that free quarks may be infinitely massive, while constituent quarks weigh about 1/3 of the proton mass, and current quarks, which play a role in deep inelastic scattering, weigh only a few MeV/c^2, is discussed in Reference 9 and also by Weinberg.[10] Although no one knows how to calculate these effects, the explanation is believed to lie in the interaction between the quark and the color gluon field. A free quark has a gluon field which has nowhere to terminate, and whose energy increases with distance. Moving the quark requires moving the field, which makes the quark very heavy. Constituent quarks in a baryon have a place to terminate their gluon fields not far away, and are thus not very heavy. Deep inelastic scattering presumably hits a single quark so hard and so fast that the gluon field does not recoil, thus showing the "true" quark mass. It would clearly be desirable to calculate all this in QCD.

Various QCD effects, such as contributions due to sea quarks, may be expected to alter the simple broken SU_6 predictions for the baryon magnetic moments. Indeed, as seen from the Table, neither the Ξ^- nor the Ξ° result is in very good agreement with the model. The experimental value for μ_{Ξ° is three standard deviations too small in magnitude. It is obviously desirable to improve the experimental accuracy with which μ_{Σ^+}, μ_{Ξ^-}, and μ_{Σ^-} are known.

In previous work the Σ^+ [11] and Ξ^- [12] moments have been measured at lower hyperon momentum, using an exclusive reaction to produce the polarization. Very strong magnetic fields - the order of 100 kg - were needed to precess the spin because of the short hyperon flight path. The angular distribution of daughter baryons in the parent hyperon center of mass, $N(\theta) = 1/2\ (1 + \alpha P \cos\theta)$, was used to measure the direction of the hyperon spin as a function of precession magnetic field. Here θ is the polar angle between the initial hyperon spin vector P and the daughter baryon momentum, and α is the asymmetry parameter, a constant for a given hyperon decay mode. The decay $\Sigma^+ \rightarrow p\pi^\circ$ fortunately has $\alpha_+ = -1$, and is a very sensitive analyzer of the Σ^+ spin direction. The asymmetry parameter for $\Xi^- \rightarrow \Lambda\pi^-$, $\alpha_{\Xi^-} = -0.4$, is smaller, but adequate. As a rule of thumb, the amount of data required to measure the hyperon spin direction to a given accuracy depends inversely on the square of α. The only non-leptonic decay mode of the Σ^-, $\Sigma^- \rightarrow n\pi^-$, has an asymmetry parameter $\alpha_- = -.07$, too small to allow conventional techniques to be used to measure the magnetic moment before the availability of intense polarized hyperon beams. For this reason previous measurements of μ_{Σ^-} have been done from spin - orbit splitting of x-ray lines in Σ^--hyperon atoms.[13]

III. The Experiment

A. Charged Hyperon Production

Figure 1 shows the curved channel inserted in the hyperon sweeping magnet. A 10 mrad bend is defined by the location of the beryllium production target, the central 4 mm diameter tungsten collimator, and the 10 mm diameter output collimator. Displacement of the orbit from the neutral beam line at the output is 25 mm. The target is displaced 12.5 mm off the magnet center line so that the orbit remains entirely within the central field region, which has been carefully mapped for E-440. The collimator currently in the hyperon magnet is similar but defines a straight line. Removing one collimator and installing the other will require a few hours. Fabrication of the new collimator can be done in about two months.

Figure 2 shows an elevation view of the set-up arranged for the measurement of the Σ^+ magnetic moment. The incident proton beam will be deflected in a vertical plane and restored to the production target by the magnet M1, thus producing a hyperon polarization in the horizontal plane, suitable for precession by the vertical field of the magnet M2, which has the curved channel in it. The production angle of ±7.5 mrad displaces the incident proton beam ±18 mm above or below the center of the 4 mm diameter tungsten collimator, so that the protons which do not interact in the 1/2 interaction length beryllium target are well contained in the shielding, independent of the polarity of the magnet M2.

Charged hyperon inclusive production spectra at 7.5 mrad and 400 GeV incident proton energy have not been measured. The CERN group has measured secondary particle ratios Σ^-/π^-, Ξ^-/π^-, and Ω^-/π^- produced by 200 GeV protons on a beryllium oxide target at 2 mrad, and the Σ^+/π^+ ratio at 6 mrad for several values of x_π near $x_\pi = 0.5$. The following procedure was adopted to calculate particle fluxes through the system proposed here. The invariant inclusive cross section $Ed^3\sigma/dp^3$ $(p + Be \rightarrow Y + X)$ was assumed to scale in the variables $(x, p_\perp)$ between 200 GeV and 400 GeV. The inclusive $\Sigma^\pm$ cross sections were assumed identical to the measured Λ cross sections in this kinematic region reported by Skubic et al.[14] For Ξ^- and Ω^-, the functional form was taken from the Λ results, but the normalization was adjusted to agree with the measured CERN ratios. Pion fluxes were calculated using the formula of Bourquin and Gaillard.[15] The secondary proton flux at the target was taken to be 10 times as large as the Σ^+ flux. This procedure was compared to experimental data at a few specific points, and always agreed with the measurements within a factor of two. It agrees with the predicted spectra for the proton lab hyperon beam given by Doroba.[16]

Figure 3a shows the predicted Σ^+ spectrum available in the decay volume after transmission by the channel in M2, assuming that the central momentum of the channel is set to 200 GeV/c. This requires a field integral of 6.6 T-m, well below the 13.6 T-m maximum excitation of the magnet. The steeply falling production spectrum shifts the central momentum of the Σ^+ to about 160 GeV/c. Figure 3b shows the correlation between the bending angle of the Σ^+ and its momentum. Momentum spectra for the other particles are similar.

this mode, and the number of protons required for 10^6 events. A positively charged particle through the spectrometer and at least one γ ray conversion in the glass will serve as the trigger. Five small drift chambers with $\pm 200\mu$ resolution will be placed 1 meter apart, beginning near the output of the M2 magnet, to help measure the hyperon momentum and detect the $\Sigma^+ \to p$ vertex. The minimum decrease in momentum in the decay $\Sigma^+ \to p$ is 12%, while typical resolution on the hyperon momentum in the drift chambers is 3% (see Figure 3b). The events will be 4-constraint fits if both γ rays convert in the glass. Background from beam protons which produce π°'s in the decay volume will be negligible.

The negative beam configuration is shown in Figure 4. The lead glass will be rotated to form a neutron detector, and will be augmented by a steel and scintillator pre-calorimeter upstream, as was done in E-415 and described by Edwards et al.[17] The resulting hadron calorimeter will be eight interaction lengths thick, and about 90% efficient for detecting neutrons from $\Sigma^- \to n\pi^-$ decay. The energy resolution was reported to be σ = 13 GeV at 100 GeV (Reference 17). The negative beam trigger will be either a $\Lambda \to p\pi^-$ detected in the spectrometer, for $\Xi^- \to \Lambda\pi^-$ and $\Omega^- \to \Lambda K^-$ decays, or a low momentum π^- in the spectrometer together with a neutral in the calorimeter for $\Sigma^- \rightarrow n\pi^-$. The Ξ^- and Ω^- decays are 4-constraint fits. The Σ^- decay is a 1-constraint fit without using the neutron energy information, which supplies an extra loose constraint. Table II shows the detection efficiency for these modes, and the number of protons required on target for 10^6 events.

C. The Magnetic Moments

The present experimental values of the magnetic moment anomalies a = (g/2-1) for Σ^+, Σ^-, and Ξ^- are shown in Table III. These are derived from the numbers in Table I, which are in units of nuclear magnetons, by multiplying μ_Y/μ_N by m_Y/m_p to obtain g/2, and then subtracting one. The anomalies are the relevant numbers for this experiment because the geometry is such that the momentum and magnetic moment vectors of the hyperon are always perpendicular to the magnetic field in the channel. The relative angle between the spin and the momentum changes by an amount θ as the hyperon travels through a field integral $\int Bdl$, where

$$\theta = a_Y \frac{\int Bdl}{3.3\ m_Y} \qquad (1)$$

Here $\int Bdl$ is in T-m, and the hyperon mass m_Y is in GeV/c^2. This formula is independent of hyperon momentum, and is valid as long as $v \approx c$, a very good approximation in this experiment.

Expected θ values are large for $\int Bdl = 6.6$ T-m, the normal tune of the channel. Thus for the Σ^+, $\theta \approx 4.4$ radians, or 250°. Since the momentum bends through only 10 mrad the particles behave almost as if they were neutral, with a total magnetic moment proportional to a. Figure 5 shows how the Σ^+ spin moves in the field, and how the spin direction everywhere is reversed by rotating the production plane through 180° about the initial hyperon momentum vector - a rotation accomplished by changing the sign of the proton production angle.

After reconstruction of a particular decay event, $\Sigma^+ \rightarrow p\pi^\circ$ for example, the direction cosines ($\cos\theta_x$, $\cos\theta_y$, $\cos\theta_z$) of the daughter baryon momentum in the hyperon rest frame can be calculated. The coordinate axes, shown in Figure 5, are such that z is along the beam line, x is horizontal, and y is vertical. The components P_x, P_y, P_z of the hyperon polarization after precession in the magnetic channel can be calculated for a sample of such reconstructed events by measuring asymmetry distributions of the form

$$N(\theta_x) = 1/2(1 + \alpha P_x \cos\theta_x), \qquad (2)$$

where α is the appropriate asymmetry parameter, given in Table III. (For the decays $\Xi^- \rightarrow \Lambda\pi^-$ and $\Omega^- \rightarrow \Lambda K^-$ the daughter baryon spin direction can also be measured, in which case α in Equation (2) is replaced by $\gamma\alpha_\Lambda$. This is important in the Ω^- case, where α is known to be small.)

Parity conservation requires $P_y = 0$. The components P_x and P_z can be reversed by reversing the production angle. The precession angle θ of Equation (1) is directly related to arctan (P_x/P_z). A straightforward calculation gives an error $\delta\theta = \frac{\delta P}{P}$, where for N events $\delta P = \frac{1}{\alpha}\sqrt{\frac{3}{N}}$ is the error in the measurement of a single component of the polarization. Equation (1) then gives an error in the anomaly $\delta a = \dfrac{10 m_Y}{\alpha\sqrt{N}}$ for a 6.6 T-m precession field integral. Taking $m_Y = 1.3$ as typical (the Ξ^- mass) and an average polarization P = .08 gives the formula $\delta a = 13/(\alpha\sqrt{N})$ which is used in Table III to compute the errors.

Geometrical biases in the apparatus which distort the distributions of the form given by Equation (2) have been calculated with Monte Carlo techniques. There is a tendency to favor daughter baryons which travel backwards in the hyperon rest frame. This is particularly true for $\Sigma^+ \to p\pi^\circ$, because the π° detection efficiency is much larger if the π° is fast in the laboratory. There is very little right-left or up-down distortion. The neutral hyperon beam group has considerable experience in handling these biases and extracting reliable polarization measurements from the data. Taking equal amounts of data with the spin in opposite directions is the key to the elimination of apparatus bias. More than one value of $\int Bdl$ will also be used to check the results.

The last column in Table III gives the anticipated errors in δa. In each case the improvement in the error is more than a factor of ten, with the exception of the Σ^-, where it is a factor of five. The Ω^- magnetic moment has never been measured.

IV. Requested Laboratory Facilities

The negative and positive charged hyperon beam runs will be done separately. About 100 hours of data at each polarity will be required to achieve the errors in Table III. A total of 300 hours in the M-2 line is requested, including tuning. A proton energy of 350 to 400 GeV and an intensity of 10^9 protons per pulse is requested. The beam spill should be 1 sec long. Three 10 foot dipoles (shown as M1 in Figure 2) are needed just upstream of the hyperon magnet to give the ±7.5 mrad production angle.

The electronics used by the neutral hyperon beam group will have to be augmented by 80 channels of drift chamber digitizer read-out which is CAMAC compatible.

The neutral hyperon beam group will supply the drift chambers, the curved channel hardware, and the modification to the lead glass to make a neutron calorimeter for $\Sigma^- \rightarrow n\pi^-$.

The experiment will be ready to run in the fall of 1979 after E-361.

References

1. L. Schachinger, et al., Phys. Rev. Lett. 41, 1348 (1978).
2. K. Heller, et al., Phys. Rev. Lett. 41, 607 (1978).
3. R. Grobel, et al., Bull. Am. Phys. Soc. 24, 46 (1979). Preliminary results from E-441.
4. G. Bunce, et al., Bull. Am. Phys. Soc. 24, 46 (1979).
5. P.T. Cox, et al., Bull. Am. Phys. Soc. 24, 636 (1979). Results from E-495.
6. P. Yamin et al., Bull. Am. Phys. Soc. 24, 46 (1979).
7. M. Bourquin, et al., contributed paper to the XIX International Conference.
8. A. DeRujula, et al., Phys. Rev. D12, 147 (1975).
9. H. Lipkin, Phys. Rev. Lett. 41, 1629 (1978).
10. S. Weinberg, Transactions of the New York Academy of Sciences - A Festschrift for II Rabi, edited by Lloyd Motz, New York, 1977 (p. 185).
11. N. Doble, et al., Phys. Lett. 67B, 483 (1977).
12. R.L. Cool, et al., Phys. Rev. D10, 792 (1974).
13. B.L. Roberts, et al., Phys. Rev. Lett. 32, 1265 (1974).
14. P. Skubic, et al., Phys. Rev. D18, 3115 (1978).
15. M. Bourquin and J.M. Gaillard, Nucl. Phys. B114, 334 (1976).
16. K. Doroba, Fermilab TM-818, 1978 (unpublished).
17. R.T. Edwards, et al., Phys. Rev. D18, 76 (1978).

Table I

Baryon Magnetic Moments

in Nuclear Magnetons $e\hbar/2m_p$

Particle	Experimental Value	Quark Model Prediction
p	2.792782 ±.000017	input
n	-1.91304211 ±.00000088	-1.86
Λ	- .6138±.0047	input
Σ^+	+ 2.83±0.25	2.67
Σ^-	- 1.48±0.37	-1.05
Ξ°	- 1.20±.06	-1.39
Ξ^-	- 1.85±.75	-0.46

The quark moments used are:

$$\mu_u = 1.862\ \mu_N$$

$$\mu_s = -.6138\ \mu_N$$

Table II

Charged Hyperon Yields

10^6 incident protons on a 15 cm long beryllium target at 7.5 mrad. Decay loss over a 6 meter flight path is included.

Particle	Yield Per 10^6 p	Average Momentum GeV/c	Decay Mode	Detection Efficiency [a]	Protons For 10^6 Events
Σ^-	1.5	150	$n\pi^-$	0.63	10^{12} [b]
Ξ^-	0.19	150	$\Lambda\pi^-$	0.26	2×10^{13} [c]
Ω^-	5×10^{-4}	160	ΛK^-	0.29	7×10^{15} [d]
π^-	2.6	150	--	--	--
Σ^+	0.8	170	$p\pi^\circ$	0.15	8×10^{12}
p	43	150	--	--	--
π^+	7.8	150	--	--	--

Notes:

a) Monte Carlo results for the indicated decay mode within the fiducial decay volume, from 6 to 16 meters from the production target.

b) Σ^- triggers will be pre-scaled by a factor of $\sim$ six and run at the same time as Ξ^-.

c) 10^9 protons per pulse and 300 pulses/hour gives 2×10^{13} in 66 hours. All detected rates at 10^9 are well within the data rate capability of the apparatus - 600 events per 1 sec spill.

d) In 2×10^{13} protons, i.e. the Ξ^- sample, there will be $\sim$ 2800 Ω^- decays.

Table III

Charged Hyperon Magnetic

Moment Anomalies

$$\mu_Y = (g/2)\ \frac{e\hbar}{2m_Y}$$

Hyperon	Experimental (g/2-1) = a±δa	Decay Mode	α	Number Of Events This Experiment	Anticipated δa[1]
Σ^+	2.62±.31	$p\pi^\circ$	-1±.02	10^6	.013
Σ^-	.89±.48	$n\pi^-$	-.069±.008	$3x10^6$	.10
Ξ^-	1.61±1.06	$\Lambda\pi^-$	-0.4±.03	10^6	.05[2]
Ω^-	(see note 3)	ΛK^-	.06±.14	2800	0.4[2]

Notes:

1. Calculated from the formula $\delta a = 13/\alpha\sqrt{N}$, which assumes an average polarization $\overline{P}_Y = 0.08$.

2. For the Ξ^- and Ω^- decays the Λ spin can be used as the analyzer so that α in the δa formula can be replaced by $\gamma\alpha_\Lambda$.

3. The broken SU_6 prediction is a = 2.28.

Figure Captions

1. Schematic of the charged hyperon channel. A central orbit with a 10 mrad bending angle is defined by the beryllium target, a central collimator, and an output collimator. The central collimator is a 4 mm diameter hole in a hevimet (tungsten alloy) plug displaced 6.6 mm from the neutral beam line. The output collimator is a 10 mm diameter hole in a hevimet plug, and is 25 mm from the beam line. The incident proton beam is a 7.5 mrad in the vertical plane, perpendicular to the plane of the drawing, and is buried in the shielding far away from the central collimator hole.

2. Elevation view of the apparatus configured for the decay $\Sigma^+ \to p\pi^\circ$. The proton beam is deflected in a vertical plane and restored to the beryllium target T by the magnet M1. M2 is the hyperon magnet, which has the curved channel of Figure 1 in it. The positive beam produced at T bends in the horizontal plane. D is an array of five small drift chambers used to measure the Σ^+ direction. V is a decay vacuum. One γ ray from the π° is shown striking a lead converter in front of chamber C3 on the face of the spectrometer magnet M3. The other γ ray converts in the lead glass array, which intercepts the same solid angle as the gap in M3. In the detail of the lead on M3, A is a veto scintillator, Pb is 2 Xrad thick, and S is a final scintillator.

Figure Captions (continued)

A lead and chamber sandwich is also used in front of the lead glass to improve the position determination of the γ rays. The hole in the lead is to allow protons to go through and strike the scintillator at P. Lead glass blocks which would be struck by the protons (two blocks in the mid plane) are also removed. This configuration of chambers, lead, and lead glass was used successfully in E-495 to detect $\Xi^\circ \to \Lambda\pi^\circ$, $\pi^\circ \to \gamma\gamma$, $\Lambda \to p\pi^-$.

3a. Momentum spectrum of transmitted Σ^+ hyperons. The peak is shifted from the central channel momentum of 200 GeV/c because the spectrum at 7.5 mrad falls rapidly with increasing lab momentum - much more rapidly than the lifetime factor.

3b. The solid line is the correlation between Σ^+ direction and momentum after the channel. The dotted curve is the θ vs p correlation for the magnet alone. A comparison of the two shows that lower momentum Σ^+'s get through the channel by way of off angle production. The slope of the straight line is 4.5 mrad in 100 GeV/c.

Figure Captions (continued)

4. Plan view of the apparatus configured for the negative beam run. The scale is the same as Figure 2. The incident proton beam is coincident with the old neutral beam direction in this view. The 10 mrad bending angle in the curved channel is distorted by the fact that the transverse scale is one-tenth the longitudinal scale. The drift chambers D are the same as Figure 2. The lead glass of Figure 2 has been rotated 90° and augmented by a steel and scintillator pre-calorimeter for neutron detection from $\Sigma^- \to n\pi^-$. Charged particles from the decay $\Xi^- \to \Lambda\pi^-$, $\Lambda \to p\pi^-$ are shown.

5a & 5b. Pictorial representation of the spin motion of the Σ^+ hyperon as it moves through the magnetic field of the hyperon precession magnet M2. Figure 5a shows the proton beam incident from below, and 5b shows it incident from above, which reverses the spin everywhere in space. The moment always precesses counter clockwise when viewed from above. The sign of the polarization shown is the same as it is for Λ production. The incident proton angle is greatly exaggerated, but the spin motion is approximately correct.

CURVED CHANNEL
NOT TO SCALE

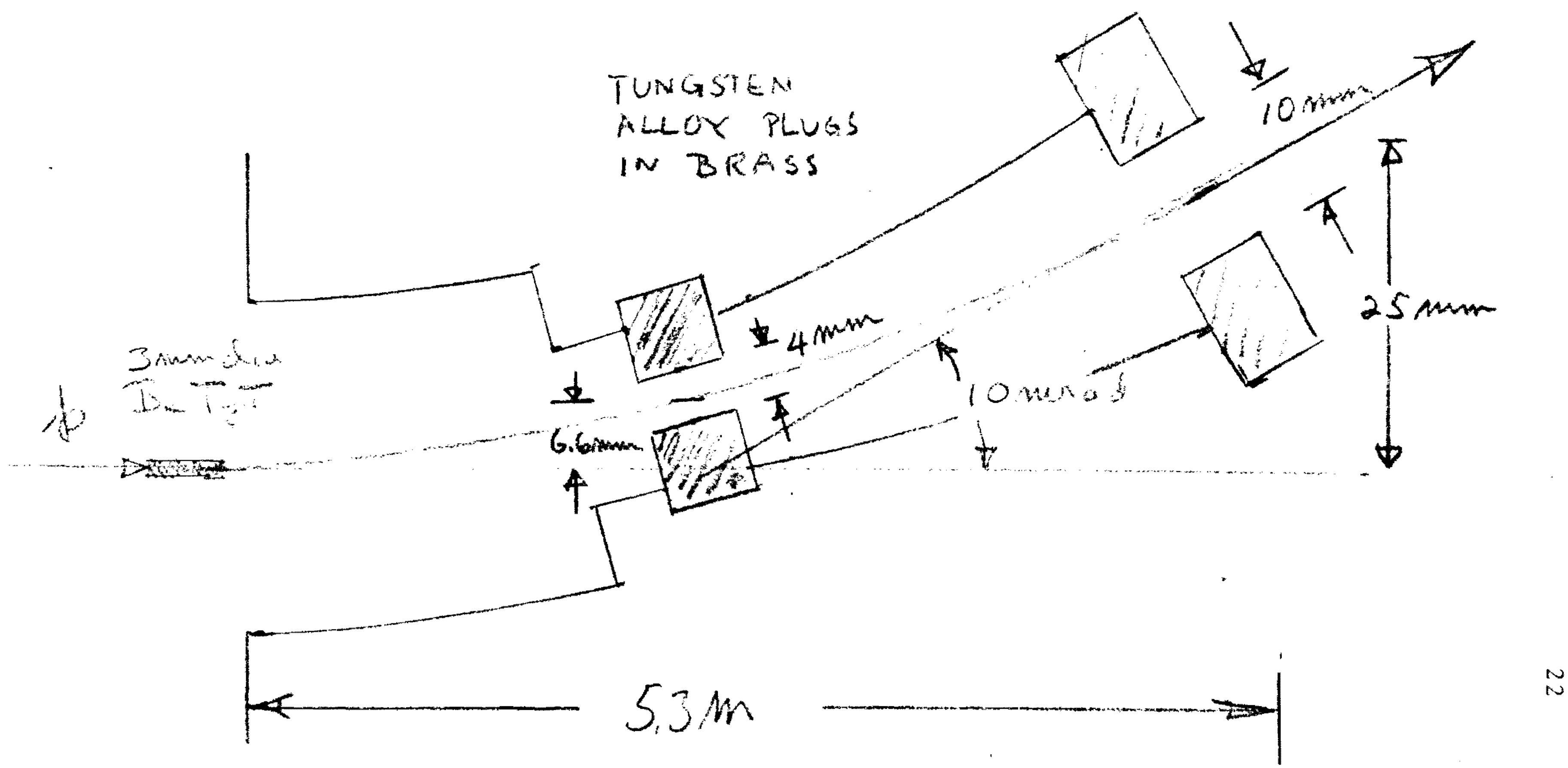

Fig 1

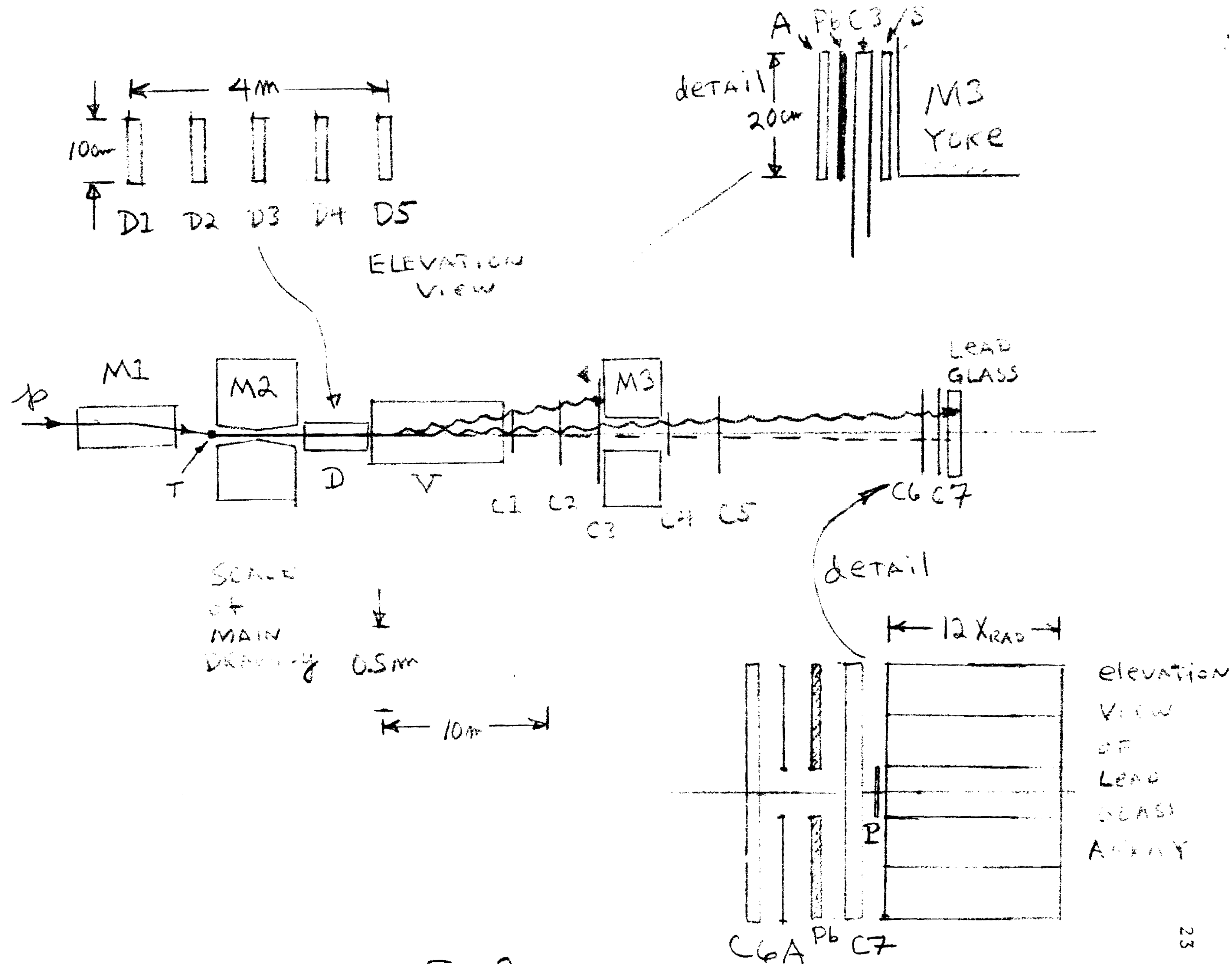

4m
100cm
D1 D2 D3 D4 D5
ELEVATION VIEW
A Pb C3 S
detail
20cm
M3 YOKE
M1
M2
M3
LEAD GLASS
p
T
D
V
C1 C2 C3 C4 C5
C6 C7
detail
SCALE of MAIN DRAWING
0.5m
10m
12 X_{RAD}
elevation view of Lead Glass Array
P
C6A Pb C7

Fig 2

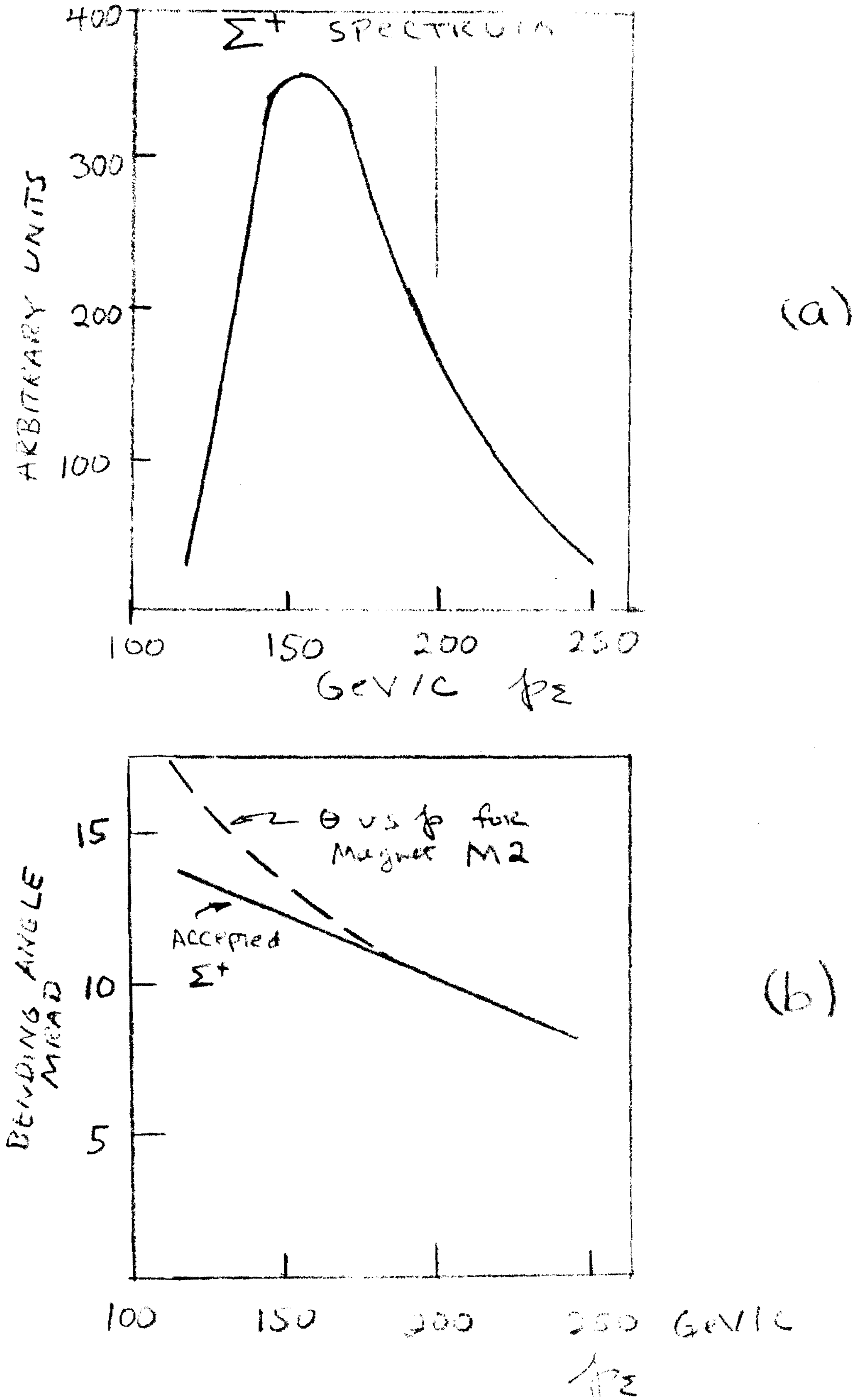

400
300
200
100
ARBITRARY UNITS
Σ+ SPECTRUM
100
150
200
250
GeV/c pΣ
(a)
θ vs p for Magnet M2
Accepted Σ+
15
10
5
BENDING ANGLE MRAD
100
150
200
250 GeV/c
pΣ
(b)

Fig 3

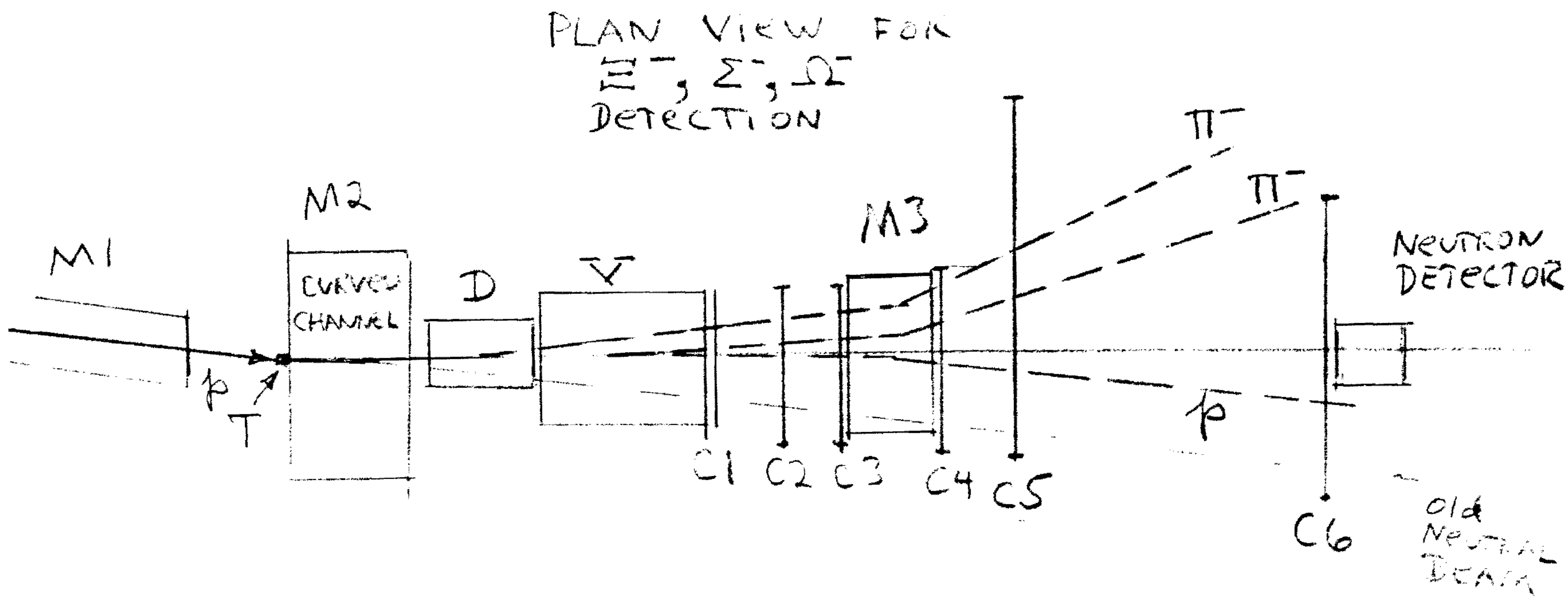
PLAN VIEW FOR
Ξ^-, Σ^-, Ω^-
DETECTION
M1
M2
CURVED CHANNEL
D
V
M3
π^-
π^-
p
T
p
C1 C2 C3 C4 C5
C6
NEUTRON DETECTOR
Old Neutral Beam

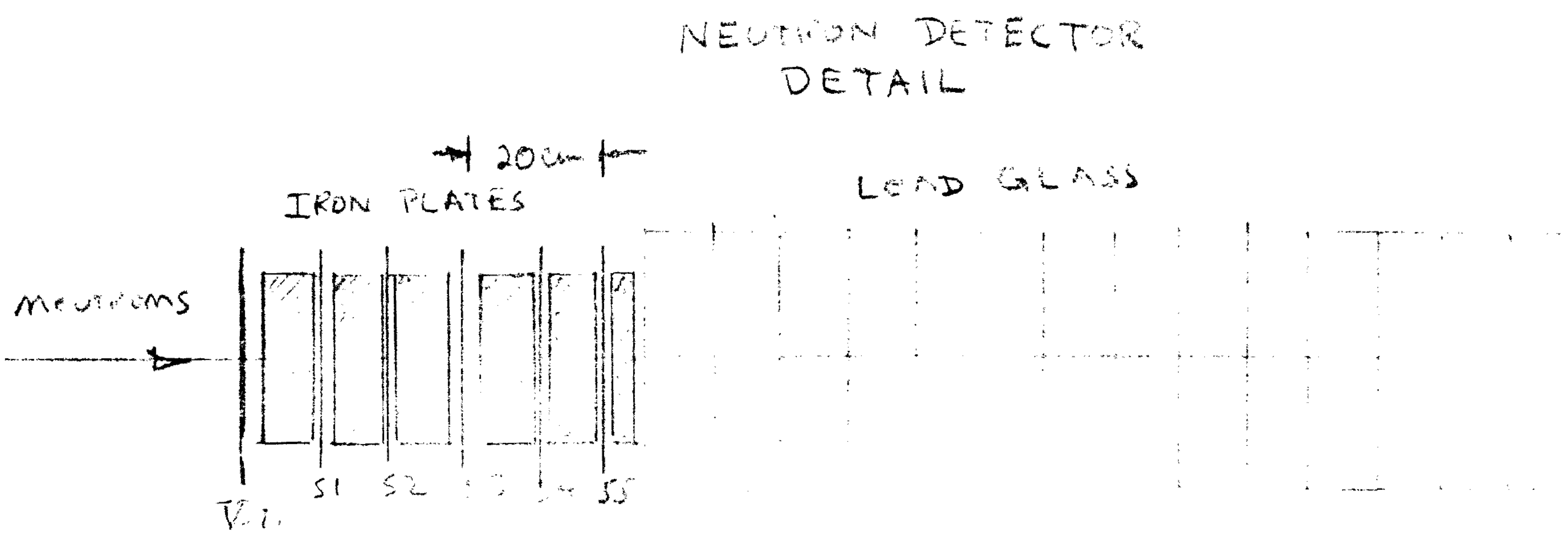
NEUTRON DETECTOR
DETAIL
20cm
IRON PLATES
LEAD GLASS
neutrons
S1 S2

Fig 4

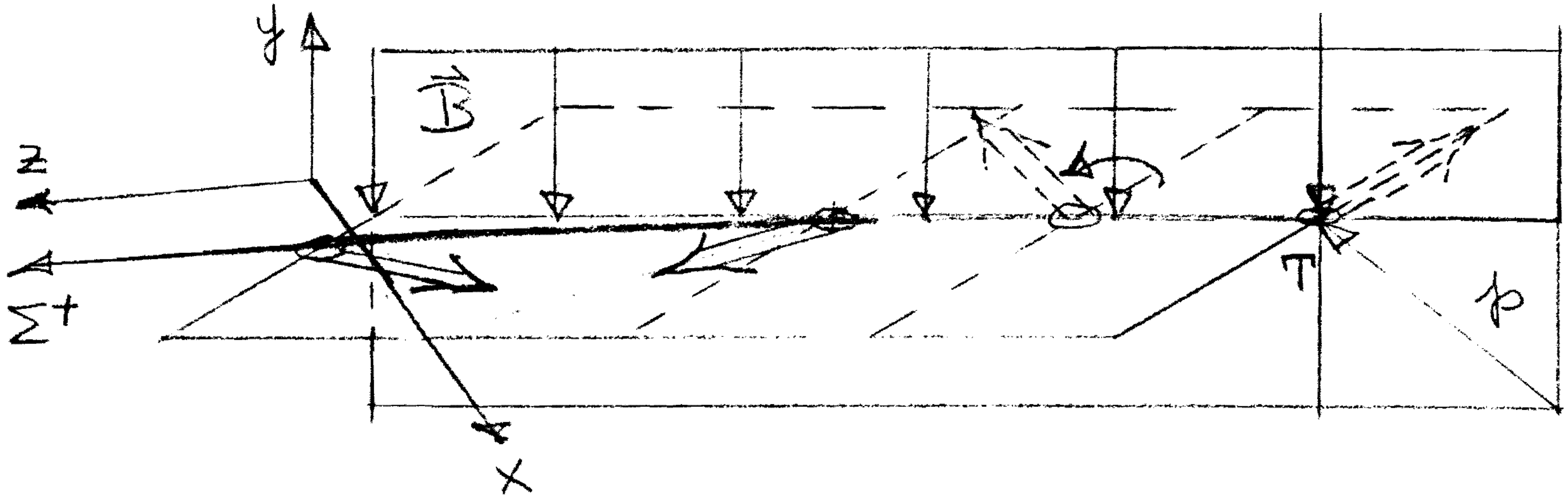

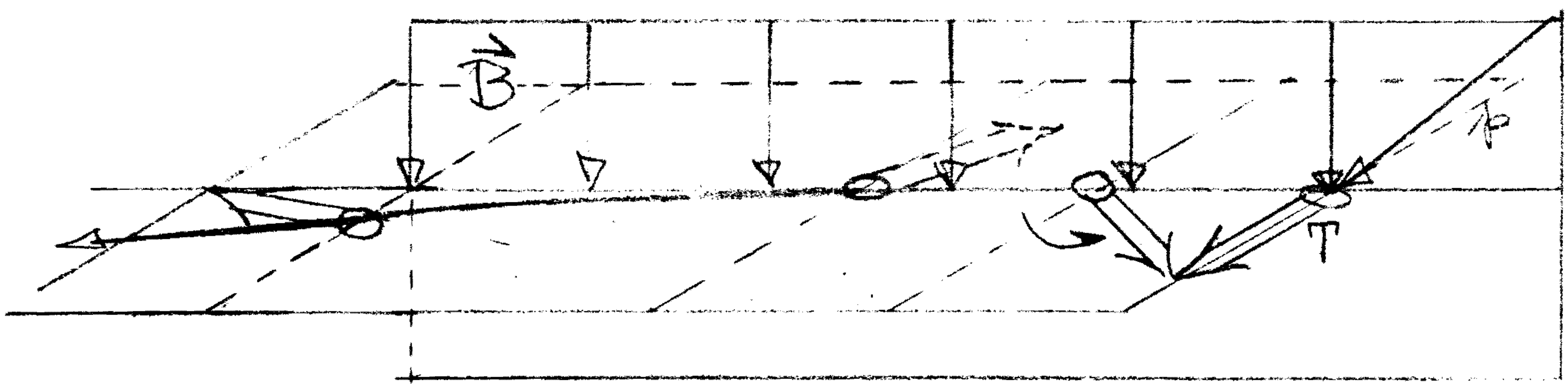

Fig 5